JOURNAL OF VIROLOGY, May 2007, p. 5132–5143 Vol. 81, No. 10
0022-538X/07/$08.00+0 doi:10.1128/JVI.02799-06

Complement Contributes to Inflammatory Tissue Destruction in a Mouse Model of Ross River Virus-Induced Disease▽

Thomas E. Morrison,[1,2,3] Robert J. Fraser,[4] Paul N. Smith,[5,6] Suresh Mahalingam,[4] and Mark T. Heise[1,2,3]*

Department of Genetics,[1] Department of Microbiology and Immunology,[2] and Carolina Vaccine Institute,[3] University of North Carolina at Chapel Hill, Chapel Hill, North Carolina 27599; Centre for Virus Research, University of Canberra, Canberra, ACT 2601, Australia[4]; Orthopedic Unit, John James Hospital, Canberra, ACT 2601, Australia[5]; and The Australian National University Medical School, Canberra, ACT 0200, Australia[6]

Received 19 December 2006/Accepted 14 February 2007

Arthritogenic alphaviruses, including Ross River virus (RRV) and chikungunya virus, are mosquito-borne viruses that cause significant human disease worldwide, including explosive epidemics that can result in thousands to millions of infected individuals. Similar to infection of humans, infection of C57BL/6 mice with RRV results in severe monocytic inflammation of bone, joint, and skeletal muscle tissues. We demonstrate here that the complement system, an important component of the innate immune response, enhances the severity of RRV-induced disease in mice. Complement activation products were detected in the inflamed tissues and in the serum of RRV-infected wild-type mice. Furthermore, mice deficient in C3 ($C3^{-/-}$), the central component of the complement system, developed much less severe disease signs than did wild-type mice. Complement-mediated chemotaxis is essential for many inflammatory arthritides; however, RRV-infected wild-type and $C3^{-/-}$ mice had similar numbers and composition of inflammatory infiltrates within hind limb skeletal muscle tissue. Despite similar inflammatory infiltrates, RRV-infected $C3^{-/-}$ mice exhibited far less severe destruction of skeletal muscle tissue. In addition to these studies, complement activation was also detected in synovial fluid from RRV-infected patients. Taken together, these findings indicate that complement activation occurs in the tissues of humans and mice infected with RRV and suggest that complement plays an essential role in the effector phase, but not the inductive phase, of RRV-induced arthritis and myositis.

Infection of humans with arthritogenic alphaviruses, such as Ross River virus (RRV), chikungunya virus, o'nyong-nyong virus, mayaro virus, and others, is a global cause of debilitating musculoskeletal disease (12, 37). These viruses are also of serious concern due to their ability to cause explosive epidemics that can involve thousands to millions of patients and potentially lead to emergence in new geographic regions. This has been highlighted by the recent epidemic reemergence of chikungunya virus in the southeastern islands of the Indian Ocean, as well as India. Since January 2005, an estimated 244,000 individuals have been infected on Réunion island alone, as well as thousands of additional cases on other islands, including Comoros, Mayotte, Seychelles, and Mauritius (34). Since many of these islands are popular tourist destinations, chikungunya virus-infected individuals returning from these areas have been identified in France, Germany, Canada, and other regions where the virus is not endemic. In addition, past epidemics include an epidemic in 1979 and 1980 of RRV disease in the South Pacific that involved more than 60,000 patients (14) and an epidemic from 1959 to 1962 of o'nyong-nyong fever in Africa that involved at least 2 million patients (41).

Humans infected with RRV, as well as other arthritogenic alphaviruses, experience disease symptoms that include fever, rash, severe muscle pain, and pain and stiffness in the joints. Treatment is palliative with anti-inflammatory drugs being the best current treatment (13, 14). RRV-induced arthritis is characterized by inflammatory infiltrates that largely consist of monocytes/macrophages (9, 15). Newly developed mouse models of alphavirus arthritis/myositis have increased our understanding of the pathogenesis of these viruses and identified host factors that contribute to the development of RRV-induced disease (26, 31). In outbred mice, RRV-induced disease was ameliorated after the treatment of mice with macrophage toxic agents, suggesting a critical role for host immunity and macrophages in mediating the disease (26). More recently, C57BL/6 (B6) wild-type and RAG-$1^{-/-}$ mice were shown to develop severe monocytic inflammation of joint, bone, and skeletal muscle tissue after RRV infection (31), supporting the concept that innate immune mechanisms play a major role and that adaptive immunity plays a more limited role in the development of RRV-induced inflammatory disease.

The complement system, which consists of greater than 30 soluble and cell surface proteins, is a major component of innate immunity that functions to recognize and eliminate invading pathogens (reviewed in reference 3). In addition, complement activation regulates downstream adaptive immune responses. The complement factor C3 functions as the central player in the complement system as the classical, lectin, and alternative complement activation pathways all converge on C3. C3 cleavage products are involved in the opsonization of pathogens, the attraction and activation of immune cells, and the amplification of complement activity through the formation of C3 and C5 convertases. In addition to the roles of the

* Corresponding author. Mailing address: The Carolina Vaccine Institute, University of North Carolina at Chapel Hill, CB #7292, Chapel Hill, NC 27599. Phone: (919) 843-1492. Fax: (919) 843-6924. E-mail: heisem@med.unc.edu.

▽ Published ahead of print on 21 February 2007.

complement system in pathogen recognition and immunoregulation, complement has been demonstrated to have a pathogenic role in ischemic, inflammatory, and autoimmune diseases.

Complement has been demonstrated to play a protective role in mouse models of some viral infections, including West Nile virus infection (28, 29) and influenza virus infection (24). However, the role of complement in alphavirus pathogenesis is less clear. In mice, complement has been shown to limit the growth and spread of the Sindbis group alphavirus AR339 (20, 22). Interestingly, complement-depleted mice also had extended survival times after lethal AR339 infection, suggesting a potential immunopathologic role for complement. In humans, studies of RRV-infected patients have thus far failed to detect evidence of immune complexes in serum or synovial exudates (10); however, alternative roles for complement in mediating disease have not been thoroughly investigated.

In the present study, we assessed the role of complement in the pathogenesis of RRV infection. Similar to wild-type mice, we found that mice deficient in C3 ($C3^{-/-}$) develop inflammation of bone, joint, and skeletal muscle tissue after RRV infection. However, despite similar virus titers, $C3^{-/-}$ mice exhibited far less severe disease signs and tissue damage compared to wild-type mice, suggesting that complement activation does not contribute to the recruitment of inflammatory cells into the RRV-infected tissues but is essential for RRV-induced damage to these tissues. Importantly, we also demonstrate that complement activation occurs in the joints of RRV-infected humans, suggesting that complement activation may play a central role in the pathogenesis of alphavirus-induced inflammatory disease.

MATERIALS AND METHODS

Viruses and cells. Viral stocks of the T48 strain of RRV were generated by in vitro transcription off of SacI-linearized plasmid pRR64 (generously provided by Richard Kuhn, Purdue University), which encodes the full-length T48 cDNA clone (25), by using SP6-specific mMessage mMachine in vitro transcription kits (Ambion). The T48 stain of RRV was initially isolated from *Aedes vigilax* mosquitoes in Queensland, Australia (8). Prior to cDNA cloning, the virus was passaged 10 times in suckling mouse brain, followed by two passages on Vero cells (6). Full-length transcripts were electroporated into BHK-21 cells (ATCC CRL 8544) by using a Bio-Rad electroporator as described previously (17). Culture supernatants were harvested 24 h after electroporation, centrifuged for 20 min at 3,000 rpm, divided into aliquots, and stored at −80°C. Virus was titrated by plaque assay on BHK-21 cells as described previously (36).

BHK-21 cells were grown in α-minimal essential medium (Gibco) supplemented with 10% donor calf serum, 10% tryptose phosphate broth, and 0.29 mg of L-glutamine/ml.

Mice. $C3^{-/-}$ and RAG-$1^{-/-}$ mice (both on the B6 background) and B6 control mice were obtained from The Jackson Laboratory (Bar Harbor, ME) and bred in house. Animal housing and care at the University of North Carolina at Chapel Hill (UNC) were in accordance with all UNC Institutional Animal Care and Use Committee guidelines. Although RRV is classified as a biosafety level 2 pathogen, due to its exotic nature all mouse studies were performed in a biosafety level 3 laboratory. Mice were inoculated in the left rear footpad with 10^3 PFU of virus in diluent (phosphate-buffered saline [PBS]–1% donor calf serum) in a 10-μl volume. Mock-infected animals received diluent alone. Mice were monitored for disease signs and weighed at 24-h intervals. The clinical signs of disease were determined by assessing grip strength and altered gait as previously described (31).

Virus titers. RRV tissue titers were determined by plaque assay on BHK-21 cells as previously described (31).

Histological analysis. Tissues were stained with hematoxylin and eosin (H&E) and analyzed as previously described (31). For the assessment of Evans blue dye (EBD) uptake into muscle fibers, 1% EBD (Sigma) in PBS (sterile-filtered) was injected into the peritoneal cavity of mock- or RRV-infected mice at various times postinfection. At 6 h postinjection, mice were perfused through the heart for 10 min with PBS–4% paraformaldehyde (pH 7.3). Quadriceps muscles were removed, embedded in optimal cutting temperature compound (Tissue-Tek), and frozen in an isopentane histobath. Cryosections were mounted with DAPI (4′,6′-diamidino-2-phenylindole)-containing Vectashield (Vector Laboratories) and analyzed by fluorescence microscopy. EBD-positive cells showed a bright red emission.

Immunoblot analysis. Dissected ankles and quadriceps skeletal muscle tissue were homogenized with 1.0-mm glass beads by using a mini-bead beater (Cole-Parmer) in radioimmunoprecipitation assay lysis buffer (50 mM Tris [pH 8.0], 150 mM NaCl, 1% Nonidet P-40, 0.5% deoxycholate, and 0.1% sodium dodecyl sulfate [SDS] supplemented with Complete protease inhibitor cocktail [Roche]). Total protein concentrations were determined by using the Coomassie Plus assay kit (Pierce). Dilutions of serum or 20 to 30 μg of protein were diluted in an equal volume of 2× SDS sample buffer, and SDS-polyacrylamide gel electrophoresis was performed. Proteins were transferred onto polyvinylidene fluoride membranes (Bio-Rad). Membranes were blocked in 1× PBS–5% milk–0.1% Tween 20 and incubated with goat anti-mouse C3 antibody (1:1,000; Cappel) overnight at 4°C or with anti-α tubulin (1:5,000; Sigma) for 1 h at room temperature. Membranes were washed in PBS–0.1% Tween 20 and incubated with rabbit anti-goat-horseradish peroxidase (1:10,000; Sigma) for 1 h at room temperature. After a washing step, proteins were visualized by enhanced chemiluminescence (Amersham) according to the manufacturer's instructions.

In situ hybridization. In situ hybridization was performed as described previously (16). Briefly, an ^{35}S-labeled RRV-specific riboprobe (complementary for RRV nucleotides 7300 to 7775) was generated with an SP6-specific MAXIscript in vitro transcription kit (Ambion) from a NotI-linearized plasmid. A riboprobe complementary for the EBER2 gene from Epstein-Barr virus was used as a negative control. Deparaffinized tissue sections were hybridized with 5×10^4 cpm of ^{35}S-labeled riboprobes/μl overnight. Tissues were washed, dehydrated through graded ethanol, and immersed in NTB autoradiography emulsion (Kodak). After development, sections were counterstained with hematoxylin, and silver grain deposition was analyzed by light microscopy.

Cytospins and flow cytometry. Mice were inoculated as described above; sacrificed by exsanguination at 5, 7, and 10 days postinfection; and perfused for 10 min with 1× PBS. Quadriceps muscles were dissected, minced, and incubated for 2 h with vigorous shaking at 37°C in digestion buffer (RPMI, 10% fetal bovine serum, 15 mM HEPES, 2.5 mg of collagenase A [Roche]/ml, 1.7 mg of DNase I [Sigma]/ml). For cytospins, a portion of the digests was deposited onto glass slides by centrifugation in the Cytofuge 2 cytocentrifuge system (StatSpin), and the cells were Wright-Giemsa stained (Sigma). For flow cytometry, cells were passed through a 70-μm-pore-size cell strainer, resuspended in 44% Percoll, layered on lympholyte-M (Cedarlane), and centrifuged for 30 min at 2,500 rpm. Banded cells were collected and washed in wash buffer (1× Hanks balanced salt solution, 15 mM HEPES), and the total viable cells were determined by trypan blue exclusion. Cells were incubated with anti-mouse FcγRII/III (2.4G2; BD Pharmingen) for 20 min on ice to block nonspecific antibody binding and then stained in fluorescence-activated cell sorting staining buffer (1× Hanks balanced salt solution, 1% fetal bovine serum, 2% normal rabbit serum) with the following antibodies from eBioscience: NK1.1-PE, CD3-fluorescein isothiocyanate, CD4-biotin, CD8α-APC, and CD11b-APC. Biotin conjugates were detected with Streptavidin-PerCP (eBioscience). Cells were fixed overnight in 2% paraformaldehyde and analyzed on a FACSCalibur (Becton Dickinson) by using CellQuest software.

Patient samples. Synovial aspirates were collected by needle biopsy from five adult male patients (age range, 30 to 45 years) suffering from acute cases of RRV-induced polyarthritis and located in the Murray-Goulburn Valley, Victoria, Australia. Collections were carried out at the Royal Melbourne Hospital, University of Melbourne, Melbourne, Australia. As a control, synovial aspirates from three osteoarthritis patients were also analyzed. Synovial aspirates from osteoarthritis patients were obtained from the John James Hospital, Canberra, Australia. All collections were performed in accordance with the Australian Capital Territory Health Community Care, Human Research Ethics, and The Royal Melbourne Hospital Human Ethics Committee and were performed by trained clinical rheumatologists. Samples were taken at the time of knee joint arthroplasty, and joints were aspirated prior to arthrotomy. Patients were diagnosed as suffering primary osteoarthritis with no evidence of an inflammatory arthropathy, and none of the patients had taken nonsteroidal anti-inflammatory drugs in the 8 weeks prior to surgery. After the collection of synovial aspirates, the cells were separated from the joint fluid by centrifugation. Synovial fluid samples were stored at −80°C befor measurement of the C3a levels.

C3a measurement. Measurement of C3a in synovial aspirates was carried out using a BD OptEIA Human C3a ELISA kit (BD Biosciences) according to the manufacturer's instructions. The mean absorbance was calculated for each set of duplicate standards, controls, and samples, and the C3a concentration of the samples was determined by using a standard curve.

Statistical analyses. Virus titers and inflammatory cell numbers were evaluated for statistically significant differences by unpaired *t* tests using GraphPad InStat3 software. For C3a analysis and clinical scores, data were statistically analyzed by the Mann-Whitney test using GraphPad InStat3 software. A P value of ≤ 0.05 was considered significant.

RESULTS

$C3^{-/-}$ mice develop less severe disease following RRV infection. Previous studies demonstrated that 24-day-old B6 mice infected with RRV developed severe disease characterized by loss of hind limb gripping ability, altered gait, and lack of weight gain, and these disease signs correlated with severe inflammation of bone, joint, and skeletal muscle tissue (31). Since complement has been shown to play an important role in inflammatory cell recruitment in numerous model systems, studies were initiated to assess the role of complement in RRV pathogenesis. 24-day-old mice deficient in the complement component C3 ($C3^{-/-}$) and control B6 mice were infected with 1000 PFU of RRV and mice were monitored for the development of disease signs. As previously reported, infection of wild-type B6 mice resulted in severe disease with peak clinical scores at day 10 (5.7 ± 0.75) and day 12 (5.8 ± 1.2) postinfection (Fig. 1A). In contrast, only very mild signs of disease were observed in RRV-infected $C3^{-/-}$ mice at day 10 (1.0 ± 0.9) and day 12 (0.7 ± 0.6) postinfection (Fig. 1A). In addition, RRV-infected B6 mice lost weight between 7 and 12 days postinfection (dpi), which correlated with peak clinical scores, whereas RRV-infected $C3^{-/-}$ mice did not lose weight at any time during the infection and in fact showed only a slightly slower rate of weight gain compared to mock-infected mice (Fig. 1B). Interestingly, the role of complement in RRV-induced disease is likely to be antibody-independent since $RAG\text{-}1^{-/-}$ mice (31), as well as μMT mice (data not shown), develop RRV disease similar to wild-type B6 mice.

Complement is activated in response to RRV infection. To determine whether the complement system was activated during RRV infection, immunoblot analyses were performed to detect C3 activation products in serum samples collected from mock-infected and RRV-infected mice at various times postinfection. C3 activation products were not detected in the serum at 2 dpi (the time point of peak virus titers in the serum) (31) or 5 dpi (data not shown). However, by 7 dpi immunoblot analyses detected an increase in fragments of αC3 in the serum, including C3d and C3c (Fig. 2A). Next, immunoblot analyses were performed on homogenates of ankle joint tissues and skeletal muscle tissues harvested from perfused mock- or RRV-infected mice. An increase in total C3 (βC3 and αC3) and a fragment of the C3 activation product iC3b were detected at 7 dpi in both ankle (Fig. 2B) and quadriceps muscle tissue (Fig. 2C) compared to mock-infected controls. The C3 activation product iC3b was also detected in joint and skeletal muscle tissues harvested from perfused RRV-infected $RAG\text{-}1^{-/-}$ mice (Fig. 2B and C), indicating that the complement system is activated in a T- and B-lymphocyte-independent manner in RRV-infected mice.

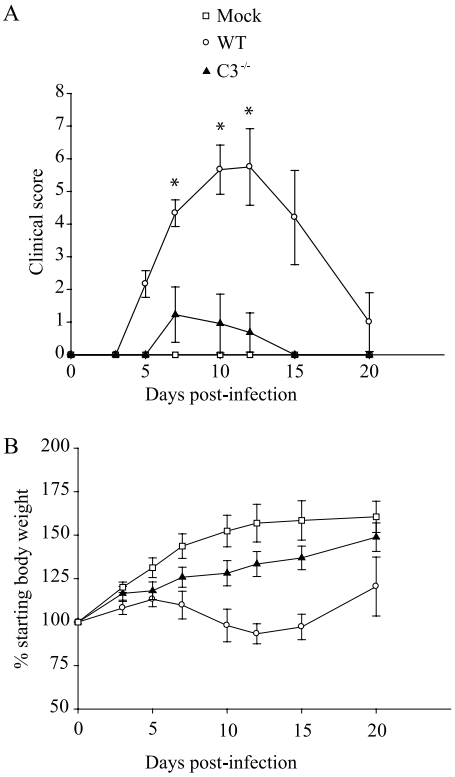

FIG. 1. RRV-induced disease is less severe in $C3^{-/-}$ mice. Twenty-four-day-old C57BL/6J wild-type (WT) or $C3^{-/-}$ mice were inoculated with 10^3 PFU of RRV by injection in the left rear footpad. Mock-infected mice were injected with diluent alone. (A) Mice were scored for the development of hind-limb dysfunction and disease based on the following scale: 0, no disease signs; 1, ruffled fur; 2, very mild hind-limb weakness; 3, mild hind-limb weakness; 4, moderate hind-limb weakness and dragging of hind limbs; 5, severe hind-limb weakness and/or dragging; 6, complete loss of hind limb function; 7, moribund; and 8, death. Each datum point represents the arithmetic mean ± the SD of 4 (mock), 6 (wild type + RRV), or 11 ($C3^{-/-}$ + RRV) mice and are representative of three independent experiments. *, $P < 0.001$. (B) Mice were monitored for weight gain or loss at 24-h intervals. Each datum point represents the arithmetic mean ± the standard deviation of 4 (mock), 6 (wild type + RRV), or 11 ($C3^{-/-}$ + RRV) mice and are representative of three independent experiments.

Viral burdens and tissue tropism are similar in wild-type and $C3^{-/-}$ mice. The primary targets of RRV replication in vivo are cells within the periosteum and synovial tissue of bone and joints, cells within the perimysium, and skeletal muscle myofibers (31). To determine whether differences in virus titers within these tissues could explain the reduced severity of disease observed in RRV-infected $C3^{-/-}$ mice, plaque assays were performed to compare the amount of infectious virus in joint and skeletal muscle tissues of RRV-infected B6 and $C3^{-/-}$ mice at 1, 2, 3, 4, and 7 dpi. Significantly higher RRV titers were detected in ankle and quadriceps muscle tissue from wild-type mice at day 1 postinfection (Fig. 3A and B), and this difference was consistent in both limbs. The only statistically significant difference detected at days 2, 3, 4, and 7 postinfection was in quadriceps muscle tissue from the right hind-limb at 3 dpi, in which $C3^{-/-}$ mice had slightly lower virus titers (Fig. 3C); however, no difference was detected in quadriceps muscle tissue from the left hind limb at this time point

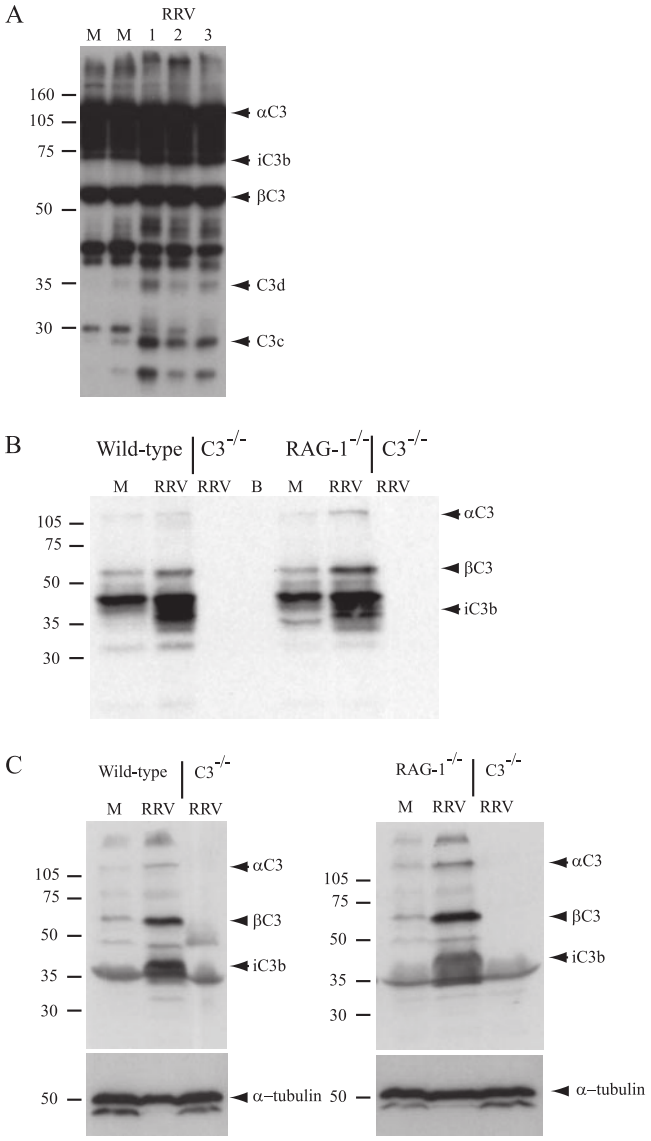

FIG. 2. Complement is activated during RRV infection. Twenty-four-day-old C57BL/6J wild-type, $C3^{-/-}$, or RAG-$1^{-/-}$ mice were infected with 10^3 PFU of RRV by injection in the left rear footpad. At 7 dpi, mice were euthanized, serum was collected, mice were perfused with 1× PBS, and the left ankle or quadriceps muscle was homogenized in radioimmunoprecipitation assay lysis buffer. Immunoblot analyses were performed with polyclonal anti-murine C3 antibody (Cappel) or an anti-α-tubulin antibody as described in Materials and Methods. (A) Serum; (B) ankle tissue; (C) quadriceps muscle tissue.

(Fig. 3B and D). Importantly, virus titers in B6 and $C3^{-/-}$ mice at 7 dpi, a time point that correlates with significant disease signs in wild-type mice, were similar in all tissues examined (Fig. 3).

The analysis of viral loads by plaque assay indicated that RRV-infected B6 and $C3^{-/-}$ mice had similar levels of viral replication within the inflamed tissues at 2, 3, 4, and 7 dpi. However, the genetic deficiency of C3 could alter viral tropism for specific cells within tissues, and this potential difference would not be detected by plaque assay. Therefore, the specific sites of RRV replication in B6 and $C3^{-/-}$ mice were assessed by in situ hybridization on sections derived from ipsilateral and contralateral (relative to injection) hind-limb tissues using an ^{35}S-labeled riboprobe specific for RRV. At 24 h postinfection (hpi), RRV-specific signal was detected within cells of the periosteum lining bones of the hind limbs and cells within synovial tissue of the ankle joint in both B6 and $C3^{-/-}$ mice (Fig. 4A). In addition, RRV-specific signal was detected in the perimysium of the quadriceps muscle of both strains of mice at 24 hpi (Fig. 4B). By 48 to 120 hpi, RRV-specific signal was detected in the skeletal muscle fibers of wild-type mice, indicating that the virus had spread from muscle connective tissues into muscle fibers. A similar distribution of RRV replication was detected in the skeletal muscle of RRV-infected $C3^{-/-}$ mice. However, at 48 hpi in $C3^{-/-}$ mice RRV-specific in situ signal was still confined to skeletal muscle connective tissues with spread into muscle fibers occurring by 72 hpi (Fig. 4B). No signal was detected in tissue sections from infected animals hybridized with a riboprobe specific for the EBER2 gene from Epstein-Barr virus (Fig. 4B) or in tissues from mock-infected animals hybridized with the RRV-specific riboprobe (data not shown). In addition, the sites of viral replication identified at each time point examined were similar in ipsilateral and contralateral tissues. These finding indicate that in the absence of C3 there may be a slight lag in muscle fiber infection, but the sites of RRV replication within hind-limb tissues were not altered.

RRV infection induces inflammation but less severe tissue destruction in $C3^{-/-}$ mice. RRV-induced inflammation in bone, joint, and skeletal muscle tissues of B6 mice is most severe at 7 to 10 dpi and resolves by 20 to 30 dpi (31). To compare tissue inflammation and pathology in RRV-infected $C3^{-/-}$ mice and control B6 mice, histological analyses of hind limb joint and skeletal muscle tissues were performed by staining fixed sections with H&E. Inflammation was not observed in synovial tissue or quadriceps skeletal muscle tissue from mock-infected mice (Fig. 5). In contrast, severe inflammation was observed in synovial tissue at 7 dpi (Fig. 5A). Inflammatory infiltrates were also observed in synovial tissue of RRV-infected $C3^{-/-}$ mice (Fig. 5A), suggesting that C3 is not required for inflammatory cell recruitment into the joints after RRV infection. Similarly, inflammatory infiltrates were also observed in quadriceps skeletal muscle tissue of RRV-infected wild-type and $C3^{-/-}$ mice at 7 and 10 dpi (Fig. 5B and C). Strikingly, despite the presence of large numbers of inflammatory infiltrates, skeletal muscle tissue pathology appeared to be much less severe in tissues from RRV-infected $C3^{-/-}$ mice than in tissues from RRV-infected wild-type mice (Fig. 5B and C). To confirm that RRV infection of $C3^{-/-}$ mice results in less severe tissue pathology, quadriceps muscle tissue was examined at 20 dpi, a time point at which inflammation has resolved but tissue damage can be observed. In RRV-infected B6 mice, numerous areas of severely damaged skeletal muscle tissue were distributed throughout the sections (Fig. 6A and B). In addition, large numbers of myofibers with centralized nuclei were evident (the hallmark of skeletal muscle regeneration) (4, 38), suggesting that wide-scale injury had taken place (Fig. 6C). In contrast, neither severely damaged areas of the skeletal muscle tissue (Fig. 6D and E) nor large numbers of myofibers with centralized nuclei (Fig. 6F) were observed in sections from the quadriceps muscle of RRV-infected $C3^{-/-}$

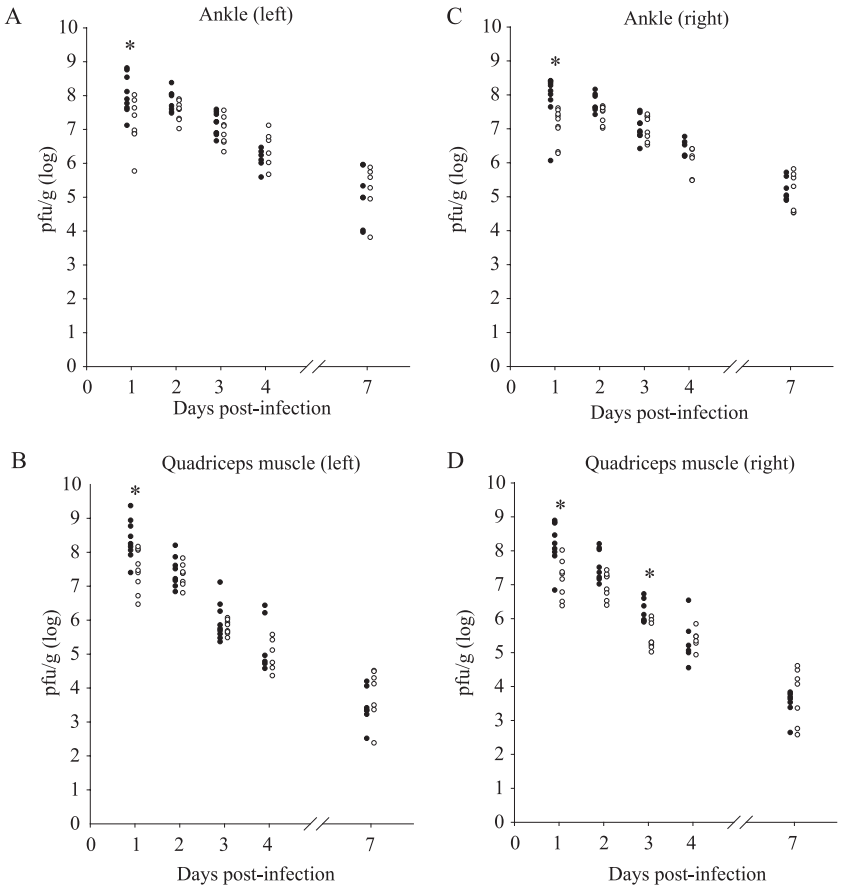

FIG. 3. RRV titers in ankle and skeletal muscle tissue. 24-day-old C57BL/6J wild-type (●) or C3$^{-/-}$ mice (○) were infected with 10^3 PFU of RRV by injection in the left rear footpad. At 1 dpi (n = 8 to 9), 2 dpi (n = 7 to 8), 3 dpi (n = 8 to 9), 4 dpi (n = 6), and 7 dpi (n = 6 to 7) the ankle and quadriceps muscle tissues were harvested and homogenized, and the amount of infectious virus present was quantified by plaque assay on BHK-21 cells. (A) Ankle (injected leg); (B) quadriceps muscle (injected leg); (C) ankle (noninjected leg); (D) quadriceps muscle (noninjected leg). The results are from two to three paired experiments, and a single animal is represented by one circle in each panel. *, $P < 0.05$.

mice at 20 dpi. These data suggest that although RRV infection induces inflammation in C3$^{-/-}$ mice similar to that observed in wild-type mice, tissue damage is much less severe. These results are consistent with the less severe disease signs observed in RRV-infected C3$^{-/-}$ mice and suggest an important role for the complement system in regulating the nature of the RRV-induced inflammatory response.

To further confirm that RRV infection results in less severe damage to skeletal muscle tissue in C3$^{-/-}$ mice compared to wild-type mice, EBD uptake was utilized to detect damaged muscle fibers in vivo. At 10 and 12 dpi (time points when RRV-induced disease signs are most severe), mock- and RRV-infected mice were injected intraperitoneally with 1% EBD. Six hours later the mice were perfused with 4% paraformaldehyde, frozen sections were generated, and EBD-positive cells (which show a bright red emission) were identified by fluorescence microscopy. Abundant EBD-positive muscle fibers were evident in sections generated from the quadriceps muscle of RRV-infected B6 mice at both 10 and 12 dpi (Fig. 7), whereas only sporadic EBD-positive fibers were detected in similar sections from RRV-infected C3$^{-/-}$ mice (Fig. 7). These data, together with the histological analyses, indicate that in the absence of an intact complement system RRV infection induces inflammation of joint and muscle tissue; however, this inflammation is far less destructive than that observed in the presence of an intact complement system.

The kinetics of inflammation and composition of inflammatory infiltrates is similar in RRV-infected wild-type and C3$^{-/-}$ mice. The histological and EBD studies suggested that RRV infection induces inflammatory infiltrates without severe tissue destruction in C3$^{-/-}$ mice. However, it is difficult to determine from these studies the total number and/or the composition of those cellular infiltrates, and changes in either could explain the difference in tissue damage observed between wild-type and C3$^{-/-}$ mice. Previous studies in humans and mice have demonstrated that RRV-induced inflammation is composed almost entirely of mononuclear infiltrates with a distinct lack of neutrophils (9, 15, 26, 31, 35). To confirm these findings, differential cell counts were performed on Giemsa-stained cytospins of collagenase-digested quadriceps muscle tissue from wild-type mice, a procedure that has been successfully used to isolate viable neutrophils (5). At 5 and 7 dpi, >98% of total leukocytes were mononuclear, and the vast majority of these cells were highly vacuolated macrophages (data not shown).

Based on these findings, the composition of mononuclear inflammatory infiltrates in wild-type and C3$^{-/-}$ mice was de-

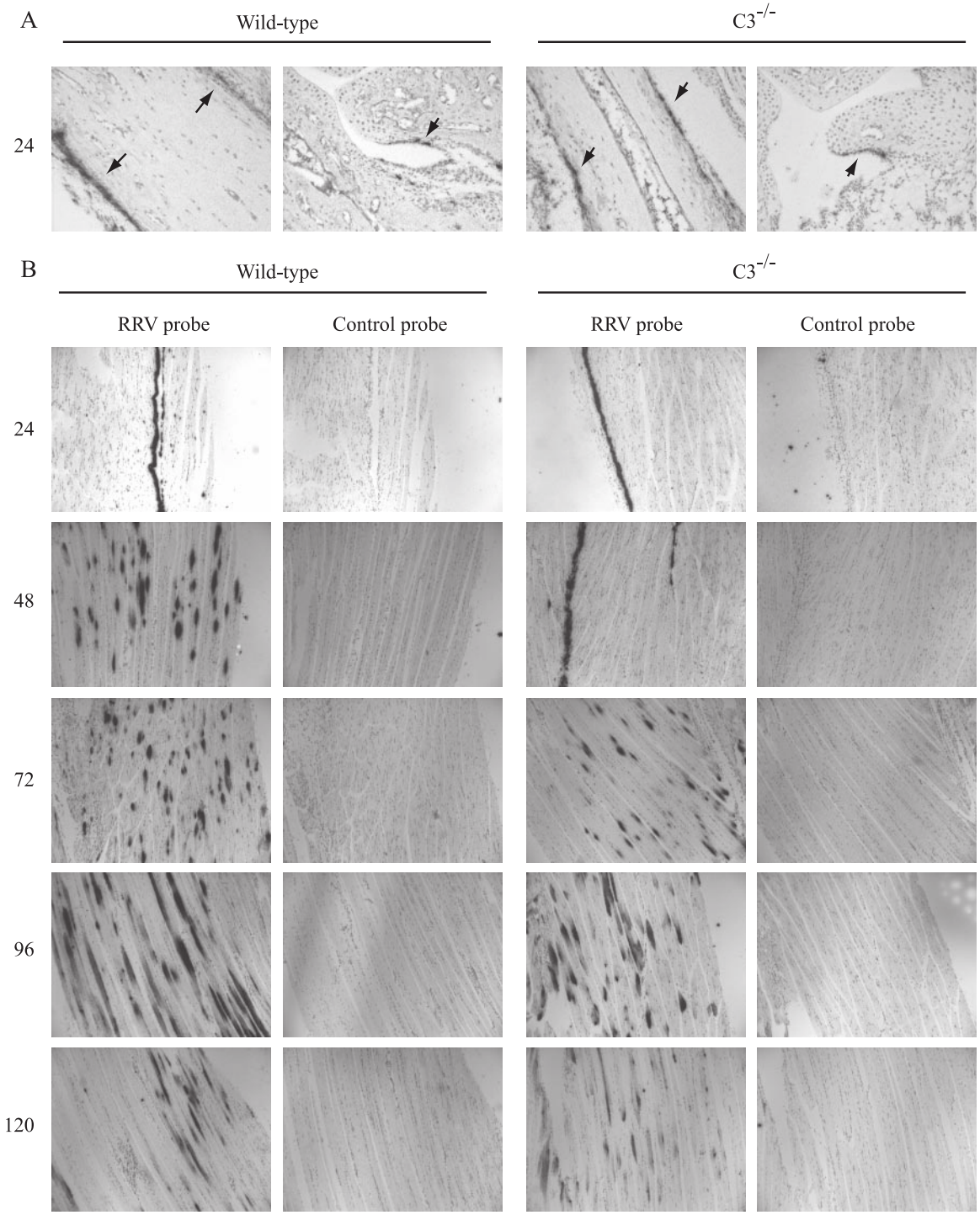

FIG. 4. RRV infection in hind limb bone, joint, and skeletal muscle. Twenty-four-day-old C57BL/6J wild-type or $C3^{-/-}$ mice were infected with 10^3 PFU of RRV by injection in the left rear footpad. Mice were sacrificed at 24, 48, 72, 96, and 120 hpi and perfused with 4% paraformaldehyde. After decalcification of calcified tissues, 5-μm-thick paraffin-embedded sections derived from the hind limbs were probed with an ^{35}S-labeled riboprobe complementary either to RRV or to the EBER2 gene from Epstein-Barr virus (control probe). (A) RRV-specific in situ signal in bones and joints of foot at 24 hpi. Two panels per strain showing signal in the periosteum (left panels) or synovial tissue (right panels) are presented. (B) RRV-specific in situ signal in quadriceps muscle tissue.

termined at various times postinfection. Single cell suspensions were generated from quadriceps muscle tissue from each of the hind limbs of RRV-infected wild-type and $C3^{-/-}$ mice. The total leukocyte numbers were determined, and isolated cells were analyzed by flow cytometry. At 5, 7, and 10 dpi no statistically significant difference in the total number of cellular inflammatory infiltrates in RRV-infected wild-type and $C3^{-/-}$ mice was detected (Fig. 8A).

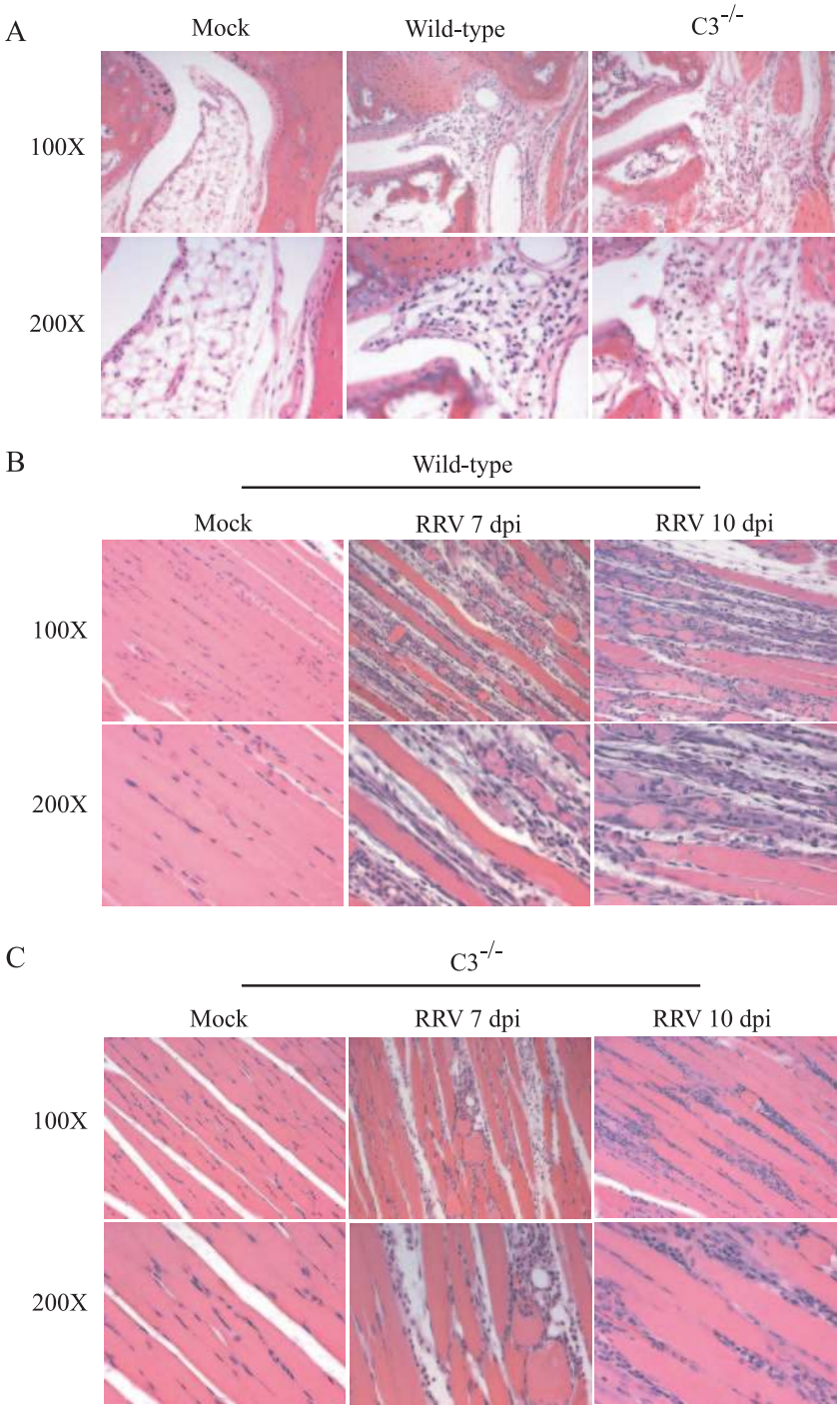

FIG. 5. RRV-induces inflammation in wild-type and $C3^{-/-}$ mice. Twenty-four-day-old C57BL/6J wild-type or $C3^{-/-}$ mice were infected with 10^3 PFU of RRV by injection in the left rear footpad. Mock-infected mice were injected with diluent alone. (A) At 7 dpi mice were perfused with 4% paraformaldehyde. After decalcification, 5-μm-thick paraffin-embedded sections generated from ankle and foot tissues of the ipsilateral and contralateral leg (relative to injection site) of mock- and RRV-infected mice were stained with H&E. The images shown are from the ipsilateral leg and are representative of at least 6 mice per group. (B and C) At 7 and 10 days postinfection mice were perfused with 4% paraformaldehyde. Paraffin-embedded sections (5-μm thick) were generated from the quadriceps muscles of mock- or RRV-infected mice as in panel A and were stained with H&E. The images are representative of at least six mice per group.

Next, flow cytometry was performed to determine the proportion of macrophages, natural killer (NK) cells, and $CD4^+$ and $CD8^+$ T lymphocytes in the inflammatory infiltrates. These cell types were previously demonstrated to comprise the majority of the RRV-induced inflammatory infiltrate (31). At 7 dpi, the percentage and total number of $CD11b^+$ inflammatory infiltrates were similar in RRV-infected wild-type and $C3^{-/-}$ mice (Fig. 8B and C and Table 1). In addition, the percentages

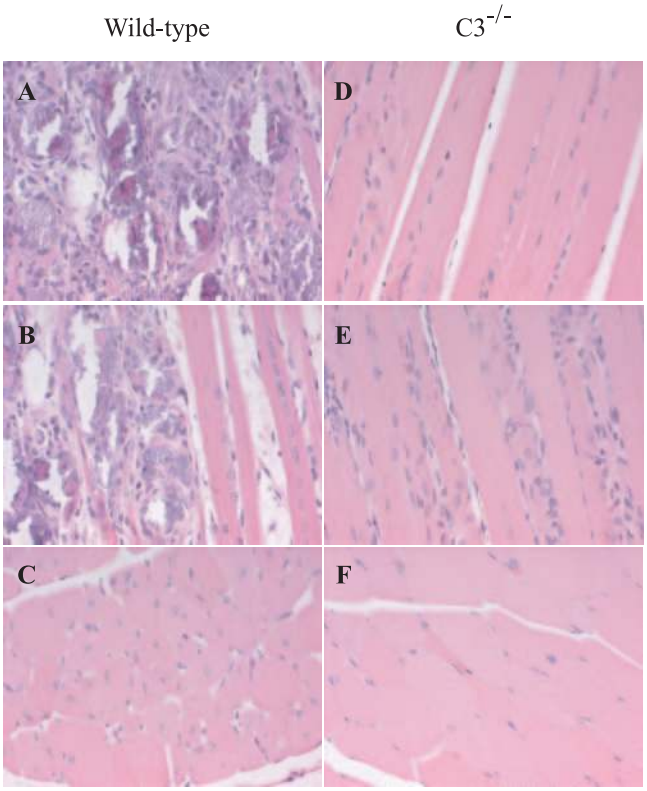

FIG. 6. Skeletal muscle damage is less severe in $C3^{-/-}$ mice. Twenty-four-day-old C57BL/6J wild-type or $C3^{-/-}$ mice were infected with 10^3 PFU of RRV by injection in the left rear footpad. At 20 dpi the mice were perfused with 4% paraformaldehyde, and 5-μm-thick paraffin-embedded sections generated from the quadriceps muscle of RRV-infected mice were stained with H&E. The images (magnification, ×200) are representative of at least six mice per group.

and total numbers of NK cells ($NK1.1^+/CD3^-$) and total $CD3^+$ T lymphocytes was also similar in RRV-infected wild-type and $C3^{-/-}$ mice (Fig. 8B, 8C, and Table 1). Interestingly, the percentage of $CD4^+$ T lymphocytes was greater in inflammatory infiltrates isolated from RRV-infected $C3^{-/-}$ mice. In contrast, RRV-infected wild-type mice had a greater percentage and greater number of $CD8^+$ T lymphocytes at this time point. The percentages and total numbers of $CD11b^+$, $NK1.1^+/CD3^-$, and $CD3^+$ cells in RRV-infected wild-type and $C3^{-/-}$ were also similar at 5 dpi (data not shown). Although a difference in a specific cell type not analyzed here cannot be ruled out, these data indicate that the overall kinetics, degree, and composition of RRV-induced inflammation are similar in wild-type and $C3^{-/-}$ mice, indicating that complement is not critical for the recruitment of cells to the inflammatory site. However, in the absence of an intact complement system, the destructive nature of the inflammation is severely attenuated.

Complement is activated in joints of RRV-infected humans. The data presented thus far suggest that the complement system contributes to the severity of RRV-induced disease in mice; however, whether complement contributes to RRV-induced disease in humans is not well understood. Although immune complexes have not been detected in RRV-infected patients, a role for complement cannot be ruled out. In this regard, the C3a levels (a marker of C3 processing) in synovial fluid from RRV patients suffering from RRV-induced polyarthritis were assessed and compared to synovial fluid from humans with noninflammatory osteoarthritis. Synovial fluid from persons suffering from acute RRV-induced polyarthritis exhibited significantly higher levels of C3a compared to samples from osteoarthritis patients (Fig. 9). Differences in C3a levels in RRV versus osteoarthritis samples were statistically significant ($P < 0.05$).

DISCUSSION

We present data here that (i) demonstrate that infection of humans and mice with RRV results in activation of the complement system and (ii) establish an important role for the complement system in inflammatory tissue damage associated with RRV infection in mice. These studies, in addition to our previous work, indicate that RRV infection of B6 mice recapitulates many aspects of the human disease and thus serves as

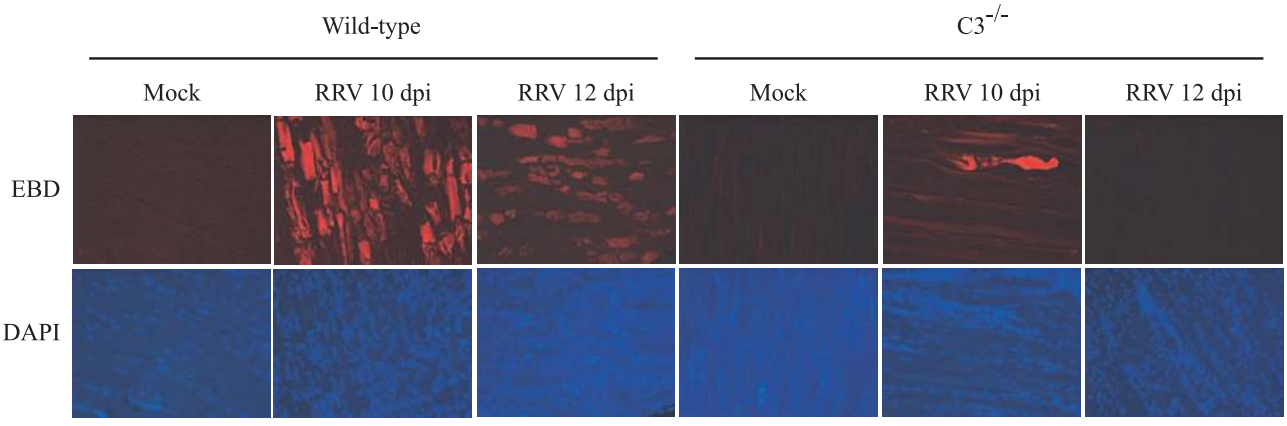

FIG. 7. RRV-induced tissue damage is less severe in $C3^{-/-}$ mice. Twenty-four-day-old C57BL/6J wild-type and $C3^{-/-}$ mice were mock infected or infected with 10^3 PFU of RRV by injection in the left rear footpad. At 10 and 12 dpi, mice were injected intraperitoneally with 1% EBD, and 6 h later mice were perfused with 4% paraformaldehyde. Quadriceps muscle tissue was removed, and 10-μm frozen sections were generated. The uptake of EBD (upper panels) and DAPI (lower panels) was visualized by fluorescence microscopy. Images (magnification, ×100) are representative of three mice per group.

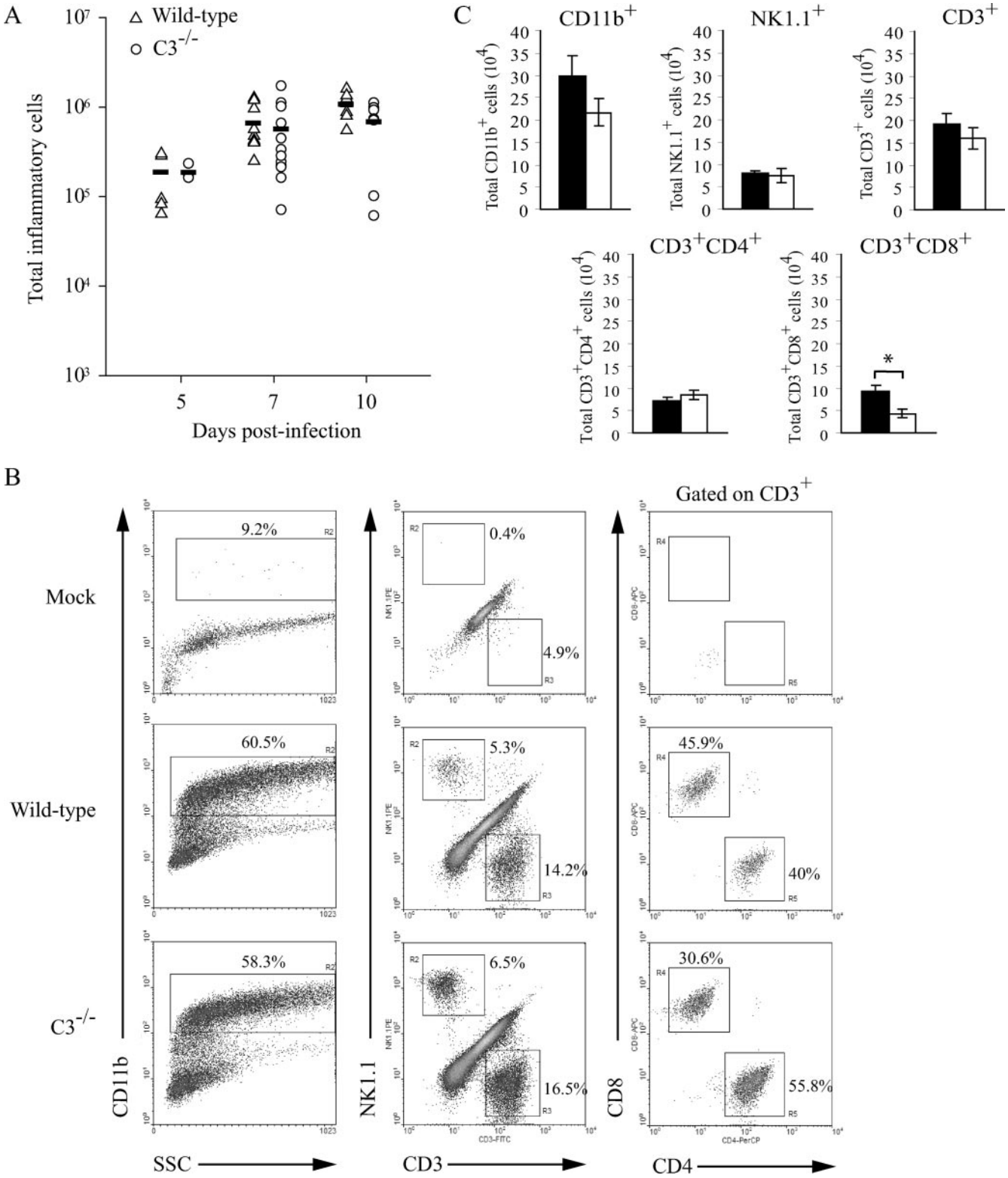

FIG. 8. Complement is not required for inflammatory cell recruitment in Ross river virus-infected mice. Twenty-four-day-old C57BL/6J WT and $C3^{-/-}$ mice were infected with 10^3 PFU of RRV by injection in the left rear footpad. (A) At 5, 7, and 10 dpi infiltrating cells were isolated from quadriceps muscle tissue as described in Materials and Methods, and the total cell number was determined. Differences were not statistically different by *t* test. (B) Cell surface staining of cells isolated from the quadriceps muscle at 7 dpi. Dot plots shown are representative of three mice. Two independent experiments gave similar results. (C) Total numbers of $CD11b^+$, $NK1.1^+/CD3^-$, $CD3^+$, $CD3^+/CD4^+$, and $CD3^+/CD8^+$ cells isolated from the quadriceps muscle of RRV-infected wild-type (■) and $C3^{-/-}$ (□) mice at 7 dpi. The data presented are the means ± the standard errors of the mean of three mice per group and are representative of two independent experiments. *, $P < 0.05$.

TABLE 1. Cell type percentages of inflammatory infiltrates

Cell type	Mean % of culture ± SD	
	Wild type	$C3^{-/-}$
$CD11b^+$	59.2 ± 4.2	55.2 ± 0.0
$NK1.1^+/CD3^-$	6.0 ± 0.4	8.0 ± 0.0
$CD3^+/NK1.1^-$	14.5 ± 0.4	16.6 ± 0.3
$CD3^+$ $CD8^+$ (% of total)	6.9 ± 0.5	5.2 ± 0.3
$CD3^+$ $CD4^+$ (% of total)	5.4 ± 0.2	9.3 ± 0.2
$CD3^+$ $CD8^+$ (% of $CD3^+$)	47.7 ± 0.4	28.5 ± 0.8
$CD3^+$ $CD4^+$ (% of $CD3^+$)	37.4 ± 0.5	56.1 ± 0.7

an accurate model to study the pathogenesis of arthritogenic alphaviruses. The contribution of complement to tissue injury in this model was independent of inflammatory cell recruitment since both wild-type and $C3^{-/-}$ mice displayed similar kinetics and compositions of cellular infiltrates at the inflammatory site.

Although complement has been reported to play a protective role in mouse models of West Nile virus infection (28, 29), influenza virus infection (24), and vesicular stomatitis virus infection (32), complement activation may be associated with more severe forms of other viral diseases, including dengue virus-induced disease and enhanced respiratory syncytial virus disease (ERD). Complement consumption has been observed in patients with dengue shock syndrome, a severe form of dengue virus infection that leads to vascular leakage, hypotension, and shock (2), and plasma SC5b-9 levels have been found to correlate with dengue hemorrhagic fever and dengue shock syndrome disease severity (1). In addition, bronchoconstriction in a mouse model of ERD was demonstrated to be complement and antibody dependent, supporting an important role for immune complex formation and complement activation in the pathogenesis of ERD (33).

In addition to our studies that implicate complement in alphavirus-induced arthritis, complement has been implicated in other mouse models of arthritic disease. Complement contributes to both the inductive phase (via C3d enhancement of B-cell responses) (7) and the inflammatory phase of type II collagen-induced arthritis. In contrast to our findings, which demonstrate a role for complement independent of inflammatory cell recruitment, complement activation in collagen-induced arthritis, as well as type II collagen MAb-induced arthritis, plays a critical role in the recruitment of cellular infiltrates into the affected joints (11, 18, 39).

Comparative analyses of the RRV-induced inflammatory infiltrates did not detect any major differences in wild-type or $C3^{-/-}$ mice with respect to kinetics, the number of infiltrating cells, or the composition of inflammatory infiltrates, although differences in a minor cellular component not examined here cannot be ruled out. Importantly, similar numbers of macrophages, the predominate cell type observed in synovial fluid of RRV-infected patients (9), were isolated from the inflamed tissue of both wild-type and $C3^{-/-}$ mice at 5 and 7 dpi. Interestingly, although similar numbers of total $CD3^+$ skeletal muscle infiltrates were detected in both strains, the percentage of $CD3^+/CD4^+$ cells was higher in RRV-infected $C3^{-/-}$ mice than in wild-type mice. Conversely, the percentage of $CD3^+/CD8^+$ cells was lower in RRV-infected $C3^{-/-}$ mice than in wild-type mice. These differences probably do not explain the difference in RRV-induced disease observed in wild-type and $C3^{-/-}$ mice, since both RAG-$1^{-/-}$ mice (31) and $CD8^{-/-}$ mice (unpublished observations) develop disease similar to that induced in wild-type mice. However, these results suggest a possible immunoregulatory role for complement during RRV-induced disease.

The histological analyses and EBD uptake studies reported here demonstrate a clear role for complement in mediating tissue injury after RRV infection. Although we cannot rule out that the differences in viral burdens detected at 1 dpi may have affected later phases of the disease, the differences in tissue injury are unlikely to be due solely to differences in viral loads since similar levels of viral replication were detected in the inflamed tissues of wild-type and $C3^{-/-}$ mice at 2, 3, 4, and 7 dpi. The mechanism(s) by which complement mediates enhanced tissue injury in RRV-infected mice is still under investigation. Beyond their well-established roles in inflammatory cell recruitment, complement activation products induce cellular activation and promote the release of potent inflammatory molecules capable of enhancing tissue destruction, including reactive oxygen intermediates and proteolytic enzymes. A previous study demonstrated that treatment of mice with macrophage toxic agents prevented development of RRV-induced disease, indicating a critical role for macrophages (26). Thus, it is possible that complement activation products regulate the effector functions of inflammatory macrophages (the predominate RRV-induced cellular infiltrate) or other cellular infiltrates by engagement of complement receptors such as CR3 or CR4. Support for a similar idea has been demonstrated in a model of thrombohemorrhagic vasculitis in which interaction of the C3 split product iC3b with CR3 expressed on infiltrating neutrophils was found to be critical for blood vessel injury (19). Alternatively, RRV-induced formation of the membrane at-

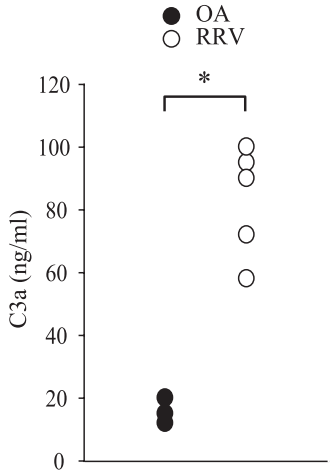

FIG. 9. C3a levels are higher in synovial fluid from humans suffering from RRV-induced polyarthritis than in synovial fluid from humans with noninflammatory osteoarthritis. Synovial fluid samples from five individuals diagnosed with acute RRV-induced polyarthritis and three individuals with osteoarthritis were assessed for C3a levels using a Human C3a EIA kit (BD Biosciences). The data are presented as mean C3a levels (in ng/ml) in synovial fluid. The differences in C3a levels in RRV versus osteoarthritis samples were statistically significant ($P < 0.05$) as determined by the Mann-Whitney U test.

tack complex, which is composed of the terminal complement components that participate directly in cell killing when present in lytic amounts, could also lead to exacerbated tissue injury.

Our immunoblot analyses in wild-type and RAG-$1^{-/-}$ mice indicate that complement activation is detectable within the injured tissues at late times postinfection. The kinetics of this activation correlates with the development of inflammation and detectable signs of disease. In addition, complement activation products were not detectable in serum from RRV-infected mice until day 7 postinfection, a time point that occurs a full 5 days after peak serum viremia. The pathway(s) by which RRV infection stimulates complement activation is currently under investigation. The detection of complement activation products in joint and muscle tissue derived from RRV-infected RAG-$1^{-/-}$ mice indicates that immune complexes are not required for RRV-induced complement activation. These findings are consistent with the lack of detection of immune complexes in synovial fluid from RRV-infected patients (10). Consistent with these findings, Sindbis virus, a related alphavirus, has been demonstrated to activate both the alternative and the classical (C4-dependent) complement activation pathways in an antibody-independent manner (23). Our preliminary results suggest that RRV-induced disease is not affected by the genetic ablation of factor B, a critical component of the alternative complement activation pathway. Therefore, there may be an important role for a lectin-dependent pathway or other C4-dependent pathways in mediating complement activation after RRV infection. Interestingly, the glycosylation status of Sindbis virus particles was shown to influence the ability of the virus to activate complement (21), suggesting that alphavirus glycoproteins may interact with the host complement system. Future studies are needed to assess the role of RRV glycoproteins and glycoprotein glycosylation in mediating RRV-induced complement activation and disease.

In addition to our studies with mice, we present evidence of complement activation in the synovial fluid of RRV-infected patients. The levels of C3a, a marker of C3 processing, were elevated in samples from RRV-infected patients compared to C3a detected in samples derived from patients diagnosed with osteoarthritis. This is the first demonstration that infection with an arthritogenic alphavirus results in complement activation within the joints. Although the role of complement in mediating joint pain in RRV-infected humans cannot be determined from these studies, these data suggest that our findings in the mouse model are consistent with at least some aspects of the human disease.

In summary, the complement system has been implicated in the pathogenesis of a number of inflammatory diseases, including other arthritides (27, 30, 40); however, the role of complement in virus-induced arthritic disease has not been well studied. The findings reported here support an important role for complement in the tissue destruction phase of RRV-induced inflammatory disease that is independent of inflammatory cell recruitment. Future studies directed at assessing the role of complement in alphavirus-induced arthritic disease in humans, such as those caused by RRV and chikungunya virus, may lead to the development of better treatments and therapeutics.

ACKNOWLEDGMENTS

This research was supported by NIH research grant R01 AR47190 and NHMRC grant 303404 (to S.M.). S.M. is the recipient of an NHMRC RD Wright Fellowship. T.E.M. was supported by NIH postdoctoral fellowship F32 AR052600-01.

We thank members of the Carolina Vaccine Institute and the Johnston laboratory for helpful scientific discussions. We thank Nancy Davis for critical reading of the manuscript. We also thank Janice Weaver, Robin Smith, and Wuhan Jiang at the LCCC/DLAM UNC histopathology core facility.

REFERENCES

1. **Avirutnan, P., N. Punyadee, S. Noisakran, C. Komoltri, S. Thiemmeca, K. Auethavornanan, A. Jairungsri, R. Kanlaya, N. Tangthawornchaikul, C. Puttikhunt, S. N. Pattanakitsakul, P. T. Yenchitsomanus, J. Mongkolsapaya, W. Kasinrerk, N. Sittisombut, M. Husmann, M. Blettner, S. Vasanawathana, S. Bhakdi, and P. Malasit.** 2006. Vascular leakage in severe dengue virus infections: a potential role for the nonstructural viral protein NS1 and complement. J. Infect. Dis. **193:**1078–1088.
2. **Bokisch, V. A., F. H. Top, Jr., P. K. Russell, F. J. Dixon, and H. J. Muller-Eberhard.** 1973. The potential pathogenic role of complement in dengue hemorrhagic shock syndrome. N. Engl. J. Med. **289:**996–1000.
3. **Carroll, M. C.** 2004. The complement system in regulation of adaptive immunity. Nat. Immunol. **5:**981–986.
4. **Charge, S. B., and M. A. Rudnicki.** 2004. Cellular and molecular regulation of muscle regeneration. Physiol. Rev. **84:**209–238.
5. **Cotter, M. J., and D. A. Muruve.** 2006. Isolation of neutrophils from mouse liver: a novel method to study effector leukocytes during inflammation. J. Immunol. Methods **312:**68–78.
6. **Dalgarno, L., C. M. Rice, and J. H. Strauss.** 1983. Ross River virus 26 s RNA: complete nucleotide sequence and deduced sequence of the encoded structural proteins. Virology **129:**170–187.
7. **Del Nagro, C. J., R. V. Kolla, and R. C. Rickert.** 2005. A critical role for complement C3d and the B-cell coreceptor (CD19/CD21) complex in the initiation of inflammatory arthritis. J. Immunol. **175:**5379–5389.
8. **Doherty, R. L., R. H. Whitehead, B. M. Gorman, and A. K. O'Gower.** 1963. The isolation of a third group A arbovirus in Australia, with preliminary observations on its relationship to epidemic polyarthritis. Aust. J. Sci. **26:** 183–184.
9. **Fraser, J. R., A. L. Cunningham, B. J. Clarris, J. G. Aaskov, and R. Leach.** 1981. Cytology of synovial effusions in epidemic polyarthritis. Aust. N. Z. J. Med. **11:**168–173.
10. **Fraser, J. R., A. L. Cunningham, J. D. Mathews, and A. Riglar.** 1988. Immune complexes and Ross River virus disease (epidemic polyarthritis). Rheumatol. Int. **8:**113–117.
11. **Grant, E. P., D. Picarella, T. Burwell, T. Delaney, A. Croci, N. Avitahl, A. A. Humbles, J. C. Gutierrez-Ramos, M. Briskin, C. Gerard, and A. J. Coyle.** 2002. Essential role for the C5a receptor in regulating the effector phase of synovial infiltration and joint destruction in experimental arthritis. J. Exp. Med. **196:**1461–1471.
12. **Griffin, D. E.** 2001. Alphaviruses, p. 917–962. *In* D. M. Knipe and P. M. Howley (ed.), Fields virology, 4th ed. Lippincott-Raven Publishers, Philadelphia, PA.
13. **Harley, D., D. Bossingham, D. M. Purdie, N. Pandeya, and A. C. Sleigh.** 2002. Ross River virus disease in tropical Queensland: evolution of rheumatic manifestations in an inception cohort followed for six months. Med. J. Aust. **177:**352–355.
14. **Harley, D., A. Sleigh, and S. Ritchie.** 2001. Ross River virus transmission, infection, and disease: a cross-disciplinary review. Clin. Microbiol. Rev. **14:** 909–932.
15. **Hazelton, R. A., C. Hughes, and J. G. Aaskov.** 1985. The inflammatory response in the synovium of a patient with Ross River arbovirus infection. Aust. N. Z. J. Med. **15:**336–339.
16. **Heise, M. T., D. A. Simpson, and R. E. Johnston.** 2000. Sindbis-group alphavirus replication in periosteum and endosteum of long bones in adult mice. J. Virol. **74:**9294–9299.
17. **Heise, M. T., L. J. White, D. A. Simpson, C. Leonard, K. A. Bernard, R. B. Meeker, and R. E. Johnston.** 2003. An attenuating mutation in nsP1 of the Sindbis-group virus S.A.AR86 accelerates nonstructural protein processing and up-regulates viral 26S RNA synthesis. J. Virol. **77:**1149–1156.
18. **Hietala, M. A., I. M. Jonsson, A. Tarkowski, S. Kleinau, and M. Pekna.** 2002. Complement deficiency ameliorates collagen-induced arthritis in mice. J. Immunol. **169:**454–459.
19. **Hirahashi, J., D. Mekala, J. Van Ziffle, L. Xiao, S. Saffaripour, D. D. Wagner, S. D. Shapiro, C. Lowell, and T. N. Mayadas.** 2006. Mac-1 signaling via Src-family and Syk kinases results in elastase-dependent thrombohemorrhagic vasculopathy. Immunity **25:**271–283.
20. **Hirsch, R. L., D. E. Griffin, and J. A. Winkelstein.** 1978. The effect of complement depletion on the course of Sindbis virus infection in mice. J. Immunol. **121:**1276–1278.

21. **Hirsch, R. L., D. E. Griffin, and J. A. Winkelstein.** 1981. Host modification of Sindbis virus sialic acid content influences alternative complement pathway activation and virus clearance. J. Immunol. **127:**1740–1743.
22. **Hirsch, R. L., D. E. Griffin, and J. A. Winkelstein.** 1980. The role of complement in viral infections. II. The clearance of Sindbis virus from the bloodstream and central nervous system of mice depleted of complement. J. Infect. Dis. **141:**212–217.
23. **Hirsch, R. L., J. A. Winkelstein, and D. E. Griffin.** 1980. The role of complement in viral infections. III. Activation of the classical and alternative complement pathways by Sindbis virus. J. Immunol. **124:**2507–2510.
24. **Kopf, M., B. Abel, A. Gallimore, M. Carroll, and M. F. Bachmann.** 2002. Complement component C3 promotes T-cell priming and lung migration to control acute influenza virus infection. Nat. Med. **8:**373–378.
25. **Kuhn, R. J., H. G. Niesters, Z. Hong, and J. H. Strauss.** 1991. Infectious RNA transcripts from Ross River virus cDNA clones and the construction and characterization of defined chimeras with Sindbis virus. Virology **182:** 430–441.
26. **Lidbury, B. A., C. Simeonovic, G. E. Maxwell, I. D. Marshall, and A. J. Hapel.** 2000. Macrophage-induced muscle pathology results in morbidity and mortality for Ross River virus-infected mice. J. Infect. Dis. **181:**27–34.
27. **Makinde, V. A., G. Senaldi, A. S. Jawad, H. Berry, and D. Vergani.** 1989. Reflection of disease activity in rheumatoid arthritis by indices of activation of the classical complement pathway. Ann. Rheum. Dis. **48:**302–306.
28. **Mehlhop, E., and M. S. Diamond.** 2006. Protective immune responses against West Nile virus are primed by distinct complement activation pathways. J. Exp. Med. **203:**1371–1381.
29. **Mehlhop, E., K. Whitby, T. Oliphant, A. Marri, M. Engle, and M. S. Diamond.** 2005. Complement activation is required for induction of a protective antibody response against West Nile virus infection. J. Virol. **79:**7466–7477.
30. **Morgan, B. P., R. H. Daniels, and B. D. Williams.** 1988. Measurement of terminal complement complexes in rheumatoid arthritis. Clin. Exp. Immunol. **73:**473–478.
31. **Morrison, T. E., A. C. Whitmore, R. S. Shabman, B. A. Lidbury, S. Mahalingam, and M. T. Heise.** 2006. Characterization of Ross River virus tropism and virus-induced inflammation in a mouse model of viral arthritis and myositis. J. Virol. **80:**737–749.
32. **Ochsenbein, A. F., D. D. Pinschewer, B. Odermatt, M. C. Carroll, H. Hengartner, and R. M. Zinkernagel.** 1999. Protective T cell-independent antiviral antibody responses are dependent on complement. J. Exp. Med. **190:**1165–1174.
33. **Polack, F. P., M. N. Teng, P. L. Collins, G. A. Prince, M. Exner, H. Regele, D. D. Lirman, R. Rabold, S. J. Hoffman, C. L. Karp, S. R. Kleeberger, M. Wills-Karp, and R. A. Karron.** 2002. A role for immune complexes in enhanced respiratory syncytial virus disease. J. Exp. Med. **196:**859–865.
34. **Schuffenecker, I., I. Iteman, A. Michault, S. Murri, L. Frangeul, M. C. Vaney, R. Lavenir, N. Pardigon, J. M. Reynes, F. Pettinelli, L. Biscornet, L. Diancourt, S. Michel, S. Duquerroy, G. Guigon, M. P. Frenkiel, A. C. Brehin, N. Cubito, P. Despres, F. Kunst, F. A. Rey, H. Zeller, and S. Brisse.** 2006. Genome microevolution of chikungunya viruses causing the Indian Ocean outbreak. PLoS Med. **3:**e263.
35. **Seay, A. R., D. E. Griffin, and R. T. Johnson.** 1981. Experimental viral polymyositis: age dependency and immune responses to Ross River virus infection in mice. Neurology **31:**656–660.
36. **Simpson, D. A., N. L. Davis, S. C. Lin, D. Russell, and R. E. Johnston.** 1996. Complete nucleotide sequence and full-length cDNA clone of S.A.AR86, a South African alphavirus related to Sindbis. Virology **222:**464–469.
37. **Suhrbier, A., and M. La Linn.** 2004. Clinical and pathologic aspects of arthritis due to Ross River virus and other alphaviruses. Curr. Opin. Rheumatol. **16:**374–379.
38. **Tidball, J. G.** 2005. Inflammatory processes in muscle injury and repair. Am. J. Physiol. Regul. Integr. Comp. Physiol. **288:**R345–R353.
39. **Wang, Y., S. A. Rollins, J. A. Madri, and L. A. Matis.** 1995. Anti-C5 monoclonal antibody therapy prevents collagen-induced arthritis and ameliorates established disease. Proc. Natl. Acad. Sci. USA **92:**8955–8959.
40. **Ward, P. A., and N. J. Zvaifler.** 1971. Complement-derived leukotactic factors in inflammatory synovial fluids of humans. J. Clin. Investig. **50:**606–616.
41. **Williams, M. C., J. P. Woodall, and J. D. Gillett.** 1965. O'nyong-nyong fever: an epidemic virus disease in East Africa. VII. Virus isolations from man and serological studies up to July 1961. Trans. R. Soc. Trop. Med. Hyg. **59:**186–197.